Fabrication of magnesium-doped porous polylactic acid microsphere for bone regeneration

Ziwei Tao[1,#], Ziyang Yuan[2,#], Dong Zhou[3,#], Lang Qin[1], Lan Xiao[4], Shihao Zhang[1], Changsheng Liu[1,], Jinzhong Zhao[2,*], Yulin Li[1,5,*]*

Key Words:
magnesium ion; osteogenesis; polylactic acid; porous microspheres

From the Contents

ABSTRACT

Biodegradable polymer microspheres that can be used as drug carriers are of great importance in biomedical applications, however, there are still challenges in controllable preparation of microsphere surface morphology and improvement of bioactivity. In this paper, firstly, poly(L-lactic acid) (PLLA) was synthesised by ring-opening polymerisation under anhydrous anaerobic conditions and further combined with the emulsion method, biodegradable PLLA microspheres (PM) with sizes ranging from 60–100 μm and with good sphericity were prepared. In addition, to further improve the surface morphology of PLLA microspheres and enhance their bioactivity, functionalised porous PLLA microspheres loaded with magnesium oxide (MgO)/magnesium carbonate ($MgCO_3$) (PMg) were also prepared by the emulsion method. The results showed that the loading of MgO/$MgCO_3$ resulted in the formation of a porous structure on the surface of the microspheres (PMg) and the dissolved Mg^{2+} could be released slowly during the degradation of microspheres. In vitro cellular experiments demonstrated the good biocompatibility of PM and PMg, while the released Mg^{2+} further enhanced the anti-inflammatory effect and osteogenic activity of PMg. Functionalised PMg not only show promise for controlled preparation of drug carriers, but also have translational potential for bone regeneration.

http://doi.org/10.12336/biomatertransl.2023.04.007

How to cite this article:
Tao, Z.; Yuan, Z.; Zhou, D.; Qin, L.; Xiao, L.; Zhang, S.; Liu, C.; Zhao, J.; Li, Y. Fabrication of magnesium-doped porous polylactic acid microsphere for bone regeneration. *Biomater Transl.* **2023**, *4*(4), 280-290.

Introduction

Biodegradable polymer microspheres have many advantages, such as good biocompatibility, low dosage and few side effects, and therefore have a wide range of applications in medical fields such as medical aesthetic fillers,[1-3] drug delivery[4, 5] and tissue engineering,[6, 7] whereas the preparation of microsphere with controlled morphological diversity remains a significant challenge.[8-10] Polylactic acid (PLA) is a biodegradable polymer approved by the U.S. Food and Drug Administration with good biocompatibility and can be absorbed by the human body after implantation,[11, 12] and is now widely used in biomedical applications as drug delivery microspheres, resorbable membranes for bone defect repair, and surgical treatment sutures.[13-17] However, the poor biological activity of PLA and the acidic degradation environment can easily cause tissue inflammation, which has significantly hindered the further application of PLA.[18-21]

Mg^{2+} is an important trace element in the human body and an important component of bones and teeth. It can regulate cell behaviour, such as improving cell adhesion and stimulating cell differentiation, and stimulate local bone formation and healing by promoting angiogenesis, thereby promoting bone regeneration. Studies found that the controlled release of Mg^{2+} promoted angiogenesis, thereby synergistically promoting *in situ* bone regeneration by developing a new magnesium

doped double crosslinked hydrogel.[22-26] Magnesium oxide (MgO) and magnesium carbonate ($MgCO_3$) are bioactive materials with good biocompatibility,[27-29] and have different rates of Mg^{2+} dissolution.[30,31] MgO and $MgCO_3$ are alkaline and can neutralise the acidic environment caused by the degradation of PLA, thus maintaining a stable pH environment,[7, 32, 33] and the loading of MgO and $MgCO_3$ changes the surface morphology of the microspheres.[34] However, when different mass ratios of MgO and $MgCO_3$ were added, the release rate of Mg^{2+} and the surface morphology of the microspheres changed accordingly,[34] therefore, an appropriate MgO/$MgCO_3$ mass ratio can effectively enhance the bioactivity of microspheres, which has a crucial impact on osteogenic transition.[35]

As shown in **Figure 1A**, poly(L-lactic acid) (PLLA) was successfully synthesised by ring-opening polymerisation, and the microspheres (PMg) loaded with MgO/$MgCO_3$ with uniform particle size and controlled morphology were prepared by the emulsion method. The loading of MgO/$MgCO_3$ led to the appearance of porous structure on the surface of the microspheres, which facilitated the interactions with the cells compared with the conventional solid PLLA.[6, 36, 37] The MgO and $MgCO_3$ could further neutralise the acidic environment generated during the degradation process of the PMg. In addition, the Mg^{2+} rich microenvironment and porous structure of PMg facilitate the migration, proliferation and differentiation of tendon-derived stem cells (TDSCs)[38] (**Figure 1B**). Therefore, this study provides an advanced strategy to synthesise microspheres with controlled morphology and bioactive properties for bone healing.

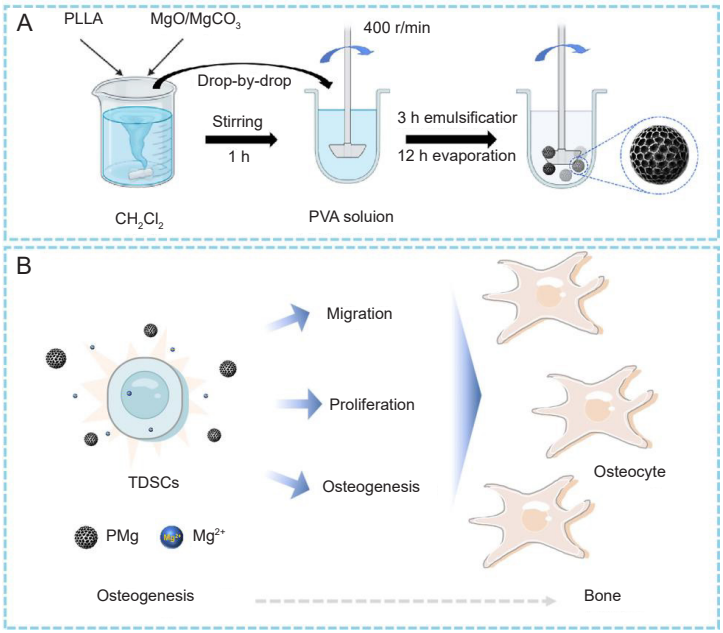

Figure 1. Schematic preparation of poly(L-lactic acid) microsphere loaded with magnesium oxide (MgO)/magnesium carbonate ($MgCO_3$) microspheres (PMg) and influence of PMg on tendon-derived stem cells (TDSCs). (A) PMg microspheres were obtained in the form of oil in water, dichloromethane (CH_2Cl_2) is the oil phase, and polyvinyl alcohol (PVA) is the water phase, the oil phase and the water phase are incompatible, so an oil-in-water system is formed, and during stirring, CH_2Cl_2 gradually evaporates, and poly(L-lactic acid) microsphere (PM) and PMg are formed. (B) PMg microspheres can maintain the continuing release of Mg^{2+} to promote the TDSC migration, proliferation, osteogenesis. Created with BioRender.com.

Methods

Synthesis of PLLA

In our previous work, we have successfully synthesised PLLA.[39] PLLA was synthesised by anhydrous and anaerobic ring-opening polymerisation, briefly, a certain amount of L-lactide (Jinan Daigang Biomaterials Co., Ltd., Jinan, China) was mixed with 0.1% $Sn(Oct)_2$ (Titan Technology Co., Ltd., Shanghai, China) in the dry flask, the temperature was raised into 140°C,

1 Engineering Research Centre for Biomedical Materials of Ministry of Education, Key Laboratory for Ultrafine Materials of Ministry of Education, School of Materials Science and Engineering, East China University of Science and Technology, Shanghai, China; 2 Department of Sports Medicine, Shanghai Sixth People's Hospital Affiliated to Shanghai Jiao Tong University School of Medicine, Shanghai, China; 3 School of Chemistry and Chemical Engineering, Nanchang University, Nanchang, Jiangxi Province, China; 4 School of Mechanical, Medical and Process Engineering, Center of Biomedical Technology, Queensland University of Technology, Brisbane, Australia; 5 Wenzhou Institute of Shanghai University, Wenzhou, Zhejiang Province, China

***Corresponding authors:**
Yulin Li, yulinli@ecust.edu.cn; Changsheng Liu, liucs@ecust.edu.cn; Jinzhong Zhao, jzzhao@sjtu.edu.cn.

#Author equally.

and the reaction was maintained in an inert atmosphere, 7 hours later, the crude products were dissolved with dichloromethane (Anhuai Chemical Technology Co., Ltd., Nantong, China), followed by precipitation in ethanol (Anhuai Chemical Technology Co., Ltd.), and then lyophilisated.

Micro-structural analysis of PLLA

The microstructure of PLLA was detected by Fourier transformed infrared spectrophotometer (Thermo Scientific, Franklin, MA, USA) in the wavelength range of 500–4000 cm^{-1}. The chemical structure of PLLA was examined by nuclear magnetic resonance spectroscopy (Bruker, Karlsruhe, UK).

Preparation of microspheres

PLLA microspheres were prepared using a previously reported method.[40] To obtain microspheres, 200 mg of PLLA was dissolved in dichloromethane and mixed with MgO/$MgCO_3$ (Shanghai Nai Cheng Biotechnology Co., Ltd., Shanghai, China), 1 hour later, the mixture was dropped into the 1% polyvinyl alcohol (Shanghai Macklin Biochemical Co., Ltd., Shanghai, China), emulsified for 3 hours, and kept stirred for overnight at room temperature to remove the dichloromethane. Finally, the collected microspheres were then washed by centrifugation three times and freeze-dried, designated as PMg. The above steps were repeated without the addition of MgO/$MgCO_3$ to obtain microspheres and named as PM.

Characterisation of microspheres

The surface morphology of microspheres was observed with a scanning electron microscope (S-3400N, Hitachi, Tokyo, Japan), and the particle size and pore size were calculated by ImageJ software (1.52t, National Institutes of Health, Bethesda, MD, USA).[41] The water contact angle of microsphere samples PM and PMg was measured using a contact angle meter (Shanghai Zhongchen Digital Technology Equipment Co., Ltd., Shanghai, China) by spreading a 1 cm × 1 cm piece of double-sided adhesive flat on a slide, then weighing the same mass of microsphere samples and spreading the microspheres uniformly and densely on the surface of the double-sided adhesive.[10] Three parallel samples were tested in each group and three different points on each parallel sample were taken for measurement.

***In vitro* degradability of microspheres**

The mass and pH value changes of the microspheres were measured to assess the degradation of microspheres in phosphate buffer saline (PBS) (Shanghai Sehan Co., Ltd., Shanghai, China). Briefly, 10 mg PM and 10 mg PMg were dispersed in 10 mL of PBS solution, stored in an incubator at 37°C and rotated at 80 r/min. The microspheres were separated from PBS at different time points (1, 3, 5, 7, 15, and 30 days), followed by determining the pH of the degradation solution of microspheres by using a pH meter (MTD, Zurich, Switzerland) and the number average molecular weight of microspheres by gel permeation chromatography. While polystyrene was used as the standard sample, and tetrahydrofuran (chromatographic grade) was used as the solvent and eluent at a flow rate of 1.0 mL/min. Finally, scanning electron microscopy was used to observe the morphological changes of the microspheres during the degradation process.

***In vitro* Mg^{2+} release from microspheres**

10 mg of PMg was immersed in 10 mL of PBS and incubated at 37 ± 1°C for 30 days. On days 1, 3, 5, 7, 15, and 30, 1 mL of sample liquid was removed and diluted to 10 mL with PBS (three parallel samples were tested at each time point), and then analysed by high-performance liquid chromatography-inductively coupled plasma mass spectrometer (NexION 2000 – (A – 10), PerkinElmer, Waltham, MA, USA).

***In vitro* cytocompatibility**

Preparation of leachate

Firstly, 10 mg of each microsphere was accurately weighed and immersed in 75% ethanol for overnight sterilisation, followed by washing the microsphere three times with PBS and twice with serum-free Dulbecco's modified Eagle medium (Gibco Life Technologies, Grand Island, NY, USA) medium, respectively. The microspheres were immersed in serum-free Dulbecco's modified Eagle medium (10 mg of microspheres:1 mL of Dulbecco's modified Eagle medium), and then placed in a thermostatic shocker (Taicang Hualida Co., Ltd., Taicang, China) at 37°C and 30 r/min for 24 hours. The leachate was collected and filtered with a 0.22-μm biofilter filtration, then 10% fetal bovine serum, 1% penicillin/streptomycin were added to prepare culture medium containing material extracts for cells.

Evaluation of cytotoxicity

All animal experiments were approved by the Ethics Committee of Shanghai Sixth People's Hospital affiliated with Shanghai Jiaotong University School of Medicine (approval No. DWSY2023-0115) on August 22, 2023. Tendon-derived stem cells (TDSCs) were isolated from the achilles tendon of 3–4-week-old male Sprague-Dawley rats (Shanghai Bikewing Biotechnology Co., Ltd., Shanghai, China) according to a previous protocol,[42] and the isolated cells were inoculated in Dulbecco's modified Eagle medium containing 10% fetal bovine serum, 1% triple antibiotic, and cultured at 37°C, 5% CO_2 environment. The medium was replaced every 2 days. The cells were passaged when they reached 80–90% confluence, and the experiments were conducted using passages 3–5 cells in this study. After 2 × 10^3 TDSCs/mL were seeded in 96-well plates, the cells were treated with the corresponding leachate for 24, 48, or 72 hours. The cells were incubated with 10 μL of CCK-8 (Beyotime, Shanghai, China) for 2 hours. The absorbance peak at 450 nm in each well was measured by a microplate reader (Molecular Device, Sunnyvale, CA, USA) to obtain the optical density (OD), and the cell viability was calculated as follows: Cell viability (%) =$100 \times \frac{OD_{experimental}}{OD_{Control}}$, where $OD_{experimental}$, and $OD_{control}$ are the optical densities for the experimental and control groups, respectively.

Live-dead staining

The cytocompatibility was evaluated by live-dead cell staining assay (Beyotime). Briefly, 5 × 10^3 TDSCs/mL were seeded in

24-well plates and placed in a 37°C, 5% CO_2 incubator for 8 hours. After the cells were adhered to the wall, the leachate of the corresponding material groups was used to treat cells for 24, 48, or 72 hours. After washing with PBS, cells were stained with calcein yellow chlorophyll and propidium iodide for 30 minutes at 37°C at 24, 48, and 72 hours. The result was observed by using confocal laser scanning microscope (Air, Tokyo, Japan).

In vitro osteogenic capacity evaluation

Alkaline phosphatase staining assay

TDSCs were seeded in 24-well plates and material-extract medium was then mixed with osteogenic medium (Beyotime) at a ratio of 1:10. After 7 days of incubation, the cells were fixed with 4% paraformaldehyde for 15 minutes, stained with alkaline phosphatase (ALP; Beyotime), stained at 37°C for 1 hour, washed twice with PBS, and photographed for observation using confocal laser scanning microscope.

Polymerase chain reaction assay

Quantitative polymerase chain reaction was tested to study the gene expression of *Arg-1* (anti-inflammatory), *Runx2* (osteogenic differentiation gene) and *Ocn* (osteogenic differentiation gene) in TDSCs. TDSCs were seeded in 6-well plates and treated with the osteogenic medium containing material leachate (1:10) for 14 days. RAW264.7 cells (Cell Bank, Chinese Academy of Science, CSTR:19375.09.3101MOUTCM13) were pretreated with 10 ng/mL lipopolysaccharides (Beyotime) for 24 hours to mimic inflammation and then incubated with extracts from each group of microspheres for 48 hours. Total RNA was isolated using the EZ pressRNA Purification kit (EZBioscience, Roseville, MN, USA) and reverse transcribed into complementary DNA using the ColorReverseTranscription kit (EZBioscience). A 10 μL reaction system was prepared using 2× SYBRGreenqPCRMasterMix (EZBioscience) and complementary DNA from each group, and quantitative polymerase chain reaction was performed on the ABI7500 polymerase chain reaction instrument (Thermo Fisher Scientific) (95°C for 30 seconds, 1 cycle; 95°C for 5 seconds; 60°C for 30 seconds, 40 cycles). The primer sequences were shown in **Table 1**. Expression levels' normalization was based on glyceraldehyde-3-phosphate dehydrogenase (*GAPDH*) expression. The gene expression level was analysed and calculated by the $2^{-\Delta\Delta Ct}$ method.[43]

Table 1. The primer sequence for polymerase chain reaction

Gene	Primer sequence (5'–3')
Arg-1	Forward: ATC AAC ACT CCG CTG ACA ACC
	Reverse: ATC TCG CAA GCC GAT GTA CAC
Runx-2	Forward: CGA ACA GAG CAA CAT CTC C
	Reverse: GTC AGT GCC TTC CTT GG
OCN	Forward: ACA AGT CCC ACA CAG CAA C
	Reverse: CCA GGT CAG AGA GGC AGA
GAPDH	Forward: CAA GAA GGT GGT GAA GCA G
	Reverse: CAA AGG TGG AAG AAT GGG

Note: Arg-1: arginase-1; GAPDH: glyceraldehyde-3-phosphate dehydrogenase; OCN: osteocalcin.

Statistical analysis

Student's unpaired *t*-test and one-way analysis of variance followed by Dunnett's multiple comparisons test were performed using GraphPad Prism (version 8.0.2 for Windows, GraphPad Software, San Diego, CA, USA, www.graphpad.com). Differences with *P* values of less than 0.05 indicated significance.

Results

Characterisation of PLLA structure

Nuclear magnetic resonance spectroscopy and Fourier transform infrared spectroscopy were used to analyse the chemical composition of PLLA. The nuclear magnetic resonance spectroscopy spectrum is depicted in **Figure 2A**, PLLA has two typical chemical shifts at 1.57 ppm and 5.17 ppm,[44] corresponding to the typical (-CH_3) and (-CH) of PLA. A typical Fourier transformed infrared spectrophotometer spectrum of PLLA is shown in **Figure 2B**, where the absorption peak at 2996 cm^{-1} corresponds to the stretching vibration of -CH in PLLA, and the absorption peaks at 1456 and 1361 cm^{-1} correspond to the bending vibration of -CH, the absorption peak at 2881 cm^{-1} corresponds to the stretching vibration of -CH_3 in PLLA; the absorption peaks at 1760 and 1187 cm^{-1} correspond to the stretching vibration of -C=O and C-O-C.[45,46] All these results indicate that PLLA has been successfully synthesised.

Characterisation of microspheres

Figure 3A and **B** depict the morphology and particle size distribution of PM and PMg under the influence of mechanical stirring, and it can be observed from scanning electron microscope images that the PM was well sphericalised, whereas the sphericalisation of PMg was slightly decreased after the addition of MgO/$MgCO_3$. Both PM and PMg showed a uniform particle size distribution (**Figure 3C** and **D**). The results suggest that there is a tendency for the particle size of the microspheres to decrease after the addition of MgO/$MgCO_3$. The particle size distribution of microspheres is shown in **Figure 3E**, and was

in the range of 60–100 μm: the particle size of PM was 82.2 ± 15.3 μm, and the particle size of PMg was 80.4 ± 14.6 μm. Infrared analysis may also be used to examine the structure of PM and PMg, and the results showed that the structure did not change considerably when compared to the raw material during the creation of microspheres (**Figure 3F**). The addition of $MgO/MgCO_3$ did not destroy the crystal structure of PLLA but further increased its crystallinity (**Additional Figure 1**).

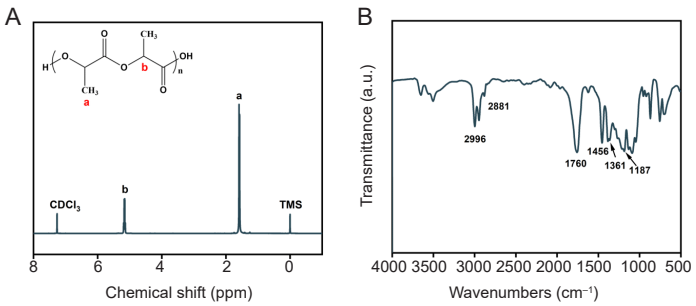

Figure 2. Chemical structure and microstructure analysis of poly(L-lactic acid) (PLLA). (A) Nuclear magnetic resonance spectroscopy, PLLA is a typical structure of polylactide, and the chemical structure of the polymer can be clearly analysed by measuring the chemical shift value of hydrogen. (B) Fourier transformed infrared spectrophotometer, the infrared visible light spectrum can clearly reflect the characteristic functional group structure in the polymer, and the polymer can be detected by the characteristic absorption peak. a.u.: arbitrary unit.

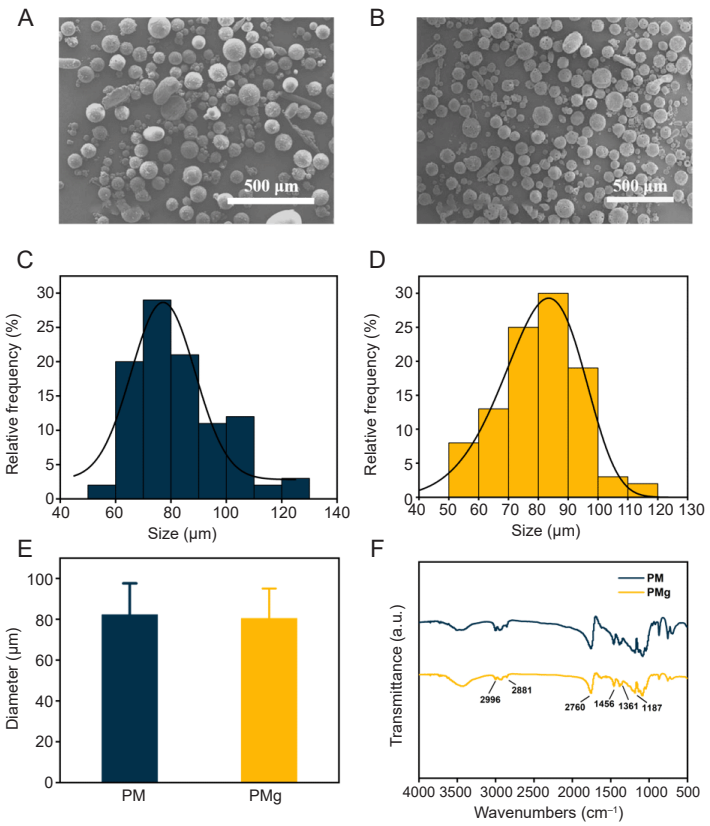

Figure 3. Characterisation of poly(L-lactic acid) microsphere (PM) and poly(L-lactic acid) microsphere loaded with magnesium oxide (MgO)/magnesium carbonate ($MgCO_3$) (PMg). (A, B) Scanning electron micrograph image of PM (A) and PMg (B). (C, D) Particle size distribution of PM (C) and PMg (D). (E) Particle size of PM and PMg. Data are expressed as mean ± SD. (F) Fourier transformed infrared spectrophotometer spectra of PM and PMg. a.u.: arbitrary unit.

Figure 4A–D display enlarged electron micrographs of PM and PMg, and the details of PM and PMg, respectively. Although the surface of PM was comparatively smooth, the addition of $MgO/MgCO_3$ resulted in the formation of numerous holes on the surface of PMg, which may have been brought on by the CO_2 production from $MgCO_3$ during the manufacturing of the microspheres. As shown statistically in **Figure 4E**, the surface of PMg produced many pore structures

with pore diameters in the range of 1–10 μm. The contact angle was measured according to previously reported work.[10] The contact angles of PM and PMg were 112.7° and 113.3° at first second, respectively. After 10 seconds of stationary, the contact angles changed to 110.2° and 103.8°, respectively. The corresponding contact angles decreased by 2.5° and 9.5°, respectively, and the decrease in the contact angle of PMg (which has a porous structure) was more obvious. This decrease may be caused by that the porous microspheres absorbed more water (**Figure 4F**).

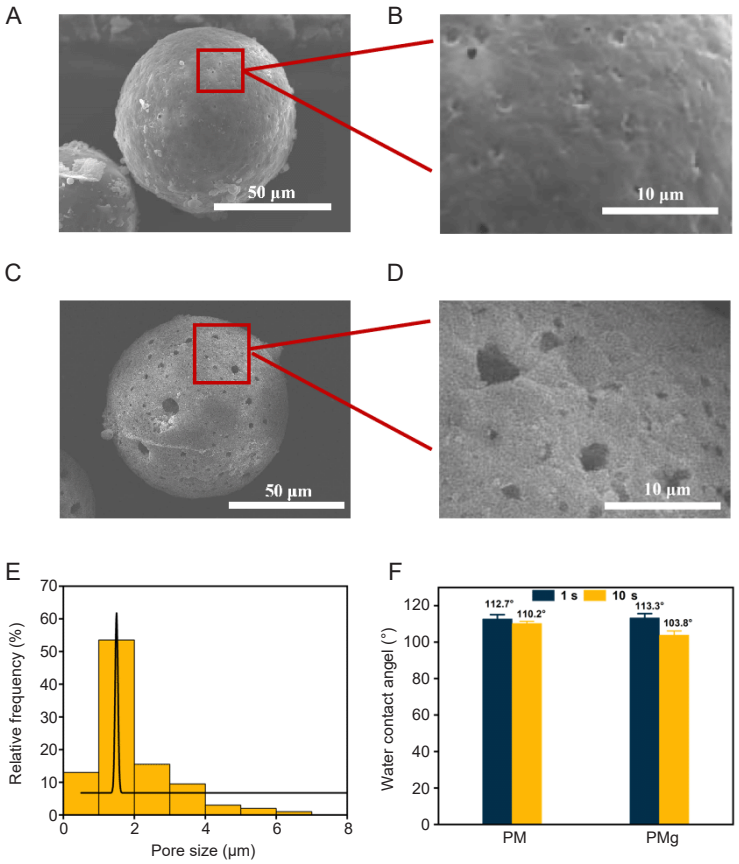

Figure 4. Enlarged microscopic images of poly(L-lactic acid) microsphere (PM) and poly(L-lactic acid) microsphere loaded with magnesium oxide (MgO)/magnesium carbonate ($MgCO_3$) (PMg). (A–D) PM surface is smooth and without porous structure, and pores appeared on the surface of PMg, which was attributed to the generation of CO_2 from $MgCO_3$. Scale bars: 50 μm (A, C), 10 μm (B, D). (E) The distribution of pore size on the surface of PMg. (F) The contact angle test of PM and PMg. PMg is more hydrophilic and absorbent compared to PM. Data are expressed as mean ± SD.

As indicated in **Figure 5A**, the number average molecular weight of PM and PMg decreased during the 30-day degradation cycle by 27.8 and 66.3 kDa, respectively, while the number average molecular weight degradation rates were 33.7% and 60.1%, respectively. These results imply that the addition of MgO and $MgCO_3$ significantly accelerates the molecular weight degradation of microspheres. As shown in **Figure 5B**, the pH of the degradation solution of PM and PMg changed from the initial 7.30 to 7.17 and 7.33, respectively, compared to PM, the pH of PMg was stabilised in the range of 7.20–7.40 during degradation, which would not interfere with the body's typical acidic and alkaline environments. As shown in **Figure 5C**, during the 30-day degradation cycle, the release of Mg^{2+} was slightly faster during the first 7 days, and the release of Mg^{2+} continued to be slow from days 7–30, and there was no burst release throughout the degradation. **Figure 5D** and **G** are scanning electron microscope images of microspheres before degradation, when degradation continued for 30 days, numbers of the "crater" structure on the PM surface increased obviously (**Figure 5E** and **F**), and the small pores on the surface of PMg gradually grew larger (**Figure 5H** and **I**).

In vitro cytocompatibility

The *in vitro* biocompatibility evaluation of the microspheres was further performed using CCK-8. As indicated in **Figure 6**, the cell survival rate was over 80% after co-cultivating the materials with TDSCs for 24, 48, and 72 hours (**Figure 6A**). The number of cells gradually increased with the increasing culture time. At 72 hours, the PMg group had the highest number of cells, indicating that the synthesised materials had no obvious inhibitory effects on cell proliferation. The live-dead staining examination revealed that the number of live cells (green) grew steadily while the number of dead cells (red) was zero, demonstrating the biocompatibility of PM and PMg (**Figure 6B**).

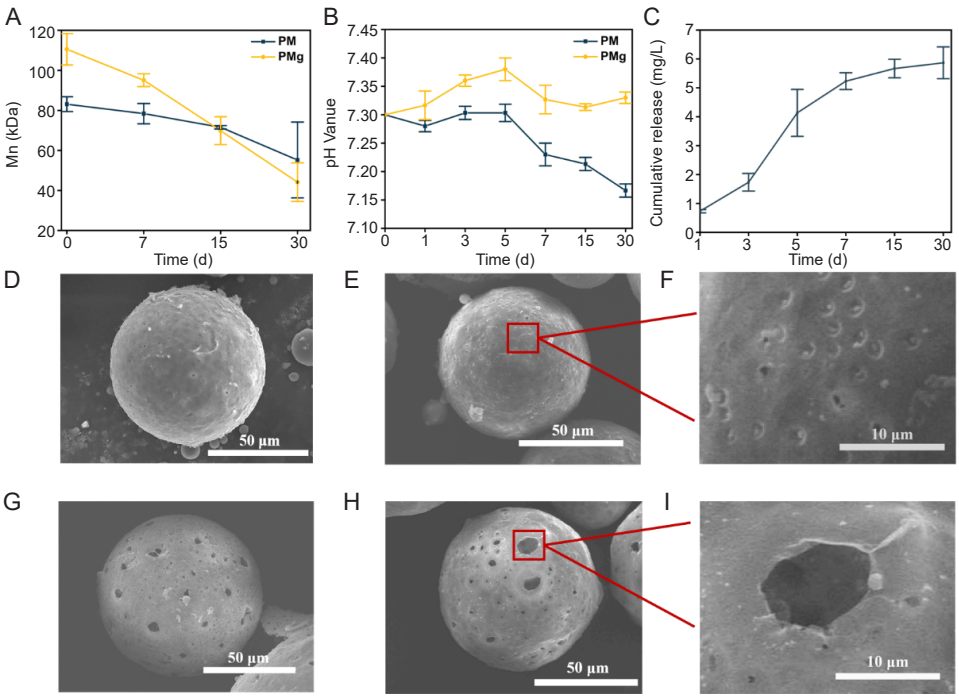

Figure 5. *In vitro* degradation behaviours of poly(L-lactic acid) microsphere (PM) and poly(L-lactic acid) microsphere loaded with magnesium oxide (MgO)/magnesium carbonate ($MgCO_3$) (PMg). (A) Accelerated degradation of PMg compared to PM, shows that MgO and $MgCO_3$ accelerate the rate of molecular weight degradation of microspheres. (B) The degradation environment pH of PMg is stable in the neutral range and does not interfere with the body's typical acidic and alkaline environment. (C) No sudden release of Mg^{2+} occurred during the 30-day degradation cycle. Data are expressed as mean ± SD, and were analysed by Student's unpaired *t*-test. (D) The scanning electron micrograph images of PM before degradation. (E) On the 30th day of degradation, scanning electron micrograph image showed that there was a significant increase in the number of "craters" on the surface of PM. (F) Enlarged scanning electron micrograph images at 30 days of PM degradation (G) The scanning electron micrograph images of PMg before degradation. (H) At 30 days of degradation, the electron micrographs showed that the pores on the surface of PMg were significantly enlarged due to corrosion. (I) Enlarged scanning electron micrograph images at 30 days of PMg degradation. Scale bars: 50 μm (D, E, G, H), 10 μm (F, I).

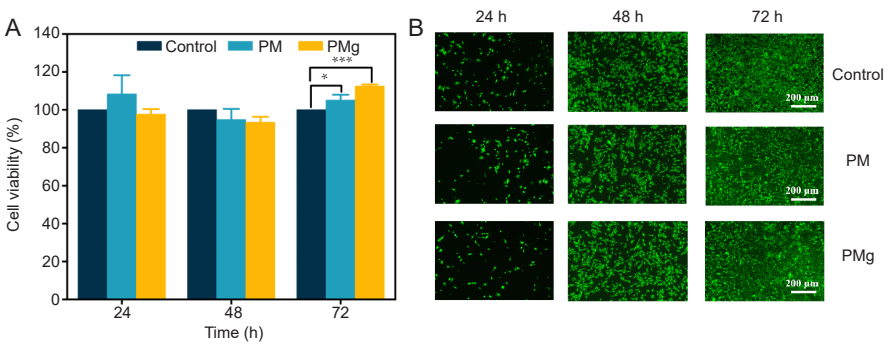

Figure 6. Cytocompatibility evaluation and live-dead staining of poly(L-lactic acid) microsphere (PM) and poly(L-lactic acid) microsphere loaded with magnesium oxide (MgO)/magnesium carbonate ($MgCO_3$) (PMg). (A) More than 80% of cell viability of tendon-derived stem cells (TDSCs) on PM and PMg, which were normalised by control group. Data are expressed as the mean ± SD ($n = 3$). *$P < 0.05$, ***$P < 0.001$ (one-way analysis of variance followed by Dunnett's multiple comparisons test). (B) Cytocompatibility of TDSCs on PM and PMg. The live/dead staining assay demonstrated that PM and PMg exhibits no cytotoxicity to cells. TDSCs cultured with osteogenic medium were used as control. Scale bars: 200 μm.

Osteogenic capacity of PM and PMg

Osteoconductive capacity is the ability of a material to support the growth of bone cells on its surface. It is an important property for bone grafts and implants, as it facilitates the integration of the material with the host bone tissue. ALP is an important biomarker of osteoblast activity. Currently, ALP activity has been used to study bone mineralisation mechanisms and bone-active biomaterials, among others.[23]

To demonstrate the osteoconductive ability of the materials, we performed a co-culture of TDSCs with the material-extract medium and evaluated ALP activity and osteogenic gene expression levels. As shown in **Figure 7A**, PM showed a stronger osteogenic capacity as indicated by the significantly higher ALP activities compared with the control, and the PMg with added MgO/$MgCO_3$ had the strongest osteogenic capacity. The above results suggest that the PLLA material had a certain osteogenic capacity,[35] and Mg^{2+} as well as the porous structure of microspheres play a more significant role in promoting the osteogenic differentiation and proliferation of TDSCs.[47] To examine the potential effect of microsphere degradation on local immune response, the expression of anti-inflammatory gene (*Arg-1*) was examined in RAW264.7 cells treated with PM and PMg, and the results showed that PMg increased the expression of *Arg-1* compared with PM (**Figure 7B**), which indicated that Mg^{2+} released from microspheres could effectively inhibit inflammation. The effects of PM and PMg on osteogenic differentiation of rat TDSCs continued to be detected by polymerase chain reaction, after 14 days of co-cultivation with the material, there was an increase in the expression of *Runx2* and *Ocn* in PM and PMg compared to the control group, whereas the gene expression in the PMg group was the highest (**Figure 7C** and **D**), which indicated that the Mg^{2+} produced by PMg group significantly enhanced the osteogenic differentiation of TDSCs.

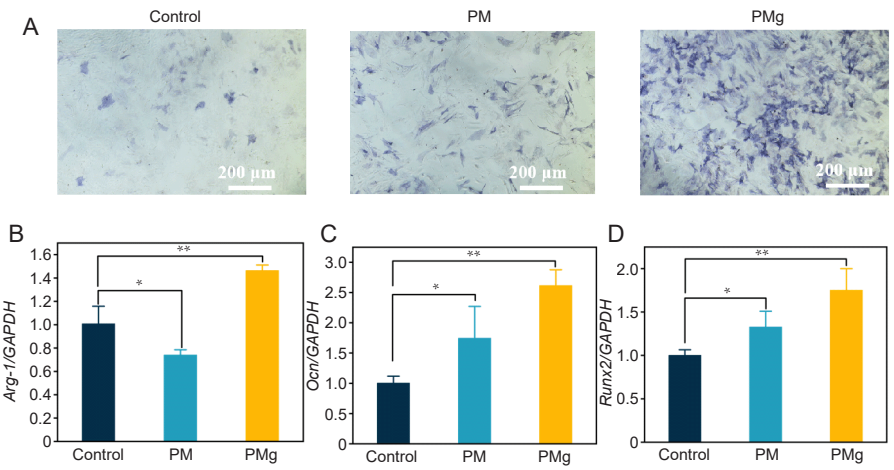

Figure 7. Osteogenic capacity evaluation of poly(L-lactic acid) microsphere (PM) and poly(L-lactic acid) (PLLA) microsphere loaded with magnesium oxide (MgO)/magnesium carbonate ($MgCO_3$) (PMg). (A) The level of alkaline phosphatase (ALP) was more obvious in PMg compared to PM. PMg has more osteogenic properties compared to PM, while PLLA material has some osteogenic properties compared to the control. (B) The expression of anti-inflammatory gene (arginase-1, *Arg-1*) was more obvious in PMg compared to PM. (C, D) The expression of osteogenic differentiation gene (osteocalcin, *Ocn*) and (*Runx2*) was more obvious in PMg compared to PM, while PLLA material can promote osteogenic differentiation of tendon-derived stem cells (TDSCs) compared to the control. RAW264.7 cells were induced with lipopolysaccharides as controls in B and TDSCs cultured with osteogenic medium were as controls in C and D. Data (normalised by control group) are expressed as the mean ± SD ($n = 3$). *$P < 0.05$, **$P < 0.01$ (one-way analysis of variance followed by Dunnett's multiple comparisons test). *GAPDH*: glyceraldehyde-3-phosphate dehydrogenase.

Discussion

PLLA was a promising U.S. Food and Drug Administration-approved biomaterial with excellent biocompatibility and degradability properties.[48] Therefore, the synthesis and application of PLLA become important, but it was a challenge to use a simple and efficient method to synthesise the PLLA and apply it to biomedical applications.[49, 50] In addition, PLLA can be prepared into different shapes and structure, and employed for biomedical applications, such as, antibacterial,[51] bone regeneration,[52] anti-inflammatory,[53] anti-tumor.[54] Among them, bioabsorbable microspheres have been widely used for drug delivery[55] and translational bone regeneration.[56]

Herein, we prepared biodegradable PLLA with good biocompatibility by a simple and green synthesis method, and porous PLLA microspheres (PMg) loaded with MgO/$MgCO_3$ have a controllable range of particle sizes using the double-emulsion method. Compared with conventional smooth microspheres, PMg has a rougher surface morphology, which facilitates cell adhesion and proliferation and increases material-cell interactions. In addition, the freeing of hydroxide ions (OH-) by PMg degradation not only neutralised the acidity of the PLLA, but also the controlled release of Mg^{2+} promoted the osteogenic differentiation of TDSCs.

Through the results of a large number of literature studies, it was found that when the microspheres were loaded with the same mass of MgO and $MgCO_3$, the optimal Mg^{2+} release rate of the microspheres was achieved,[34] therefore, this study only explored the effect of the same mass of MgO/$MgCO_3$ on the surface topography of the microspheres and the release of Mg^{2+} and did not further investigate the effect of the different mass ratios of MgO/$MgCO_3$ on the topography of the microspheres and the Mg^{2+} release rate.

In this study, we successfully prepared porous magnesium-containing microspheres with uniform particle size, combination of large and small pores, and good biocompatibility using solvent evaporation method. The average particle size of the microspheres was 60–100 μm, and the average pore size was 1–10 μm. The generation of pore structure made the surface morphology of the microspheres more controllable, which was more favorable for cell adhesion and proliferation. In addition, the slow release of Mg^{2+} during the microsphere degradation maintains a suitable concentration of Mg^{2+} at the treatment site, which inhibits inflammation and promotes the proliferation and osteogenic differentiation of osteoblasts. Therefore, this study provided an advanced strategy to prepare functionalised microspheres for bone regeneration.

Author contributions

Conceptualization, methodology, project administration and funding acquisition: CL, YL, JZ; study design, and data generation, collection, investigation, and validation: ZT, ZY; manuscript review and editing: ZT, DZ, LQ, LX, SZ. All authors approved the final version of this manuscript.

Financial support

The study was supported by National Key R&D Program of China, Nos. 2018YFE0201500, 2022YFC2405802 and National Natural Science Foundation of China, No. 51973060.

Acknowledgement

None.

Conflicts of interest statement

The authors declare no conflict of interest.

Editor note: Changsheng Liu is an Editorial Board member of *Biomaterials Translational*. He was blinded from reviewing or making decisions on the manuscript. The article was subject to the journal's standard procedures, with peer review handled independently of this Editorial Board member and his research group.

Additional file

Additional Figure 1: The X-ray powder diffraction XRD analysis of PM and PMg.

1. Cho, E. R.; Kang, S. W.; Kim, B. S. Poly(lactic-co-glycolic acid) microspheres as a potential bulking agent for urological injection therapy: preliminary results. *J Biomed Mater Res B Appl Biomater.* **2005**, *72*, 166-172.
2. Gao, Q.; Duan, L.; Feng, X.; Xu, W. Superiority of poly(l-lactic acid) microspheres as dermal fillers. *Chin Chem Lett.* **2021**, *32*, 577-582.
3. Kang, S. W.; Cho, E. R.; Jeon, O.; Kim, B. S. The effect of microsphere degradation rate on the efficacy of polymeric microspheres as bulking agents: an 18-month follow-up study. *J Biomed Mater Res B Appl Biomater.* **2007**, *80*, 253-259.
4. Zhang, M.; Tang, Y.; Zhu, Z.; Zhao, H.; Yao, J.; Sun, D. Paclitaxel and etoposide-loaded Poly (lactic-co-glycolic acid) microspheres fabricated by coaxial electrospraying for dual drug delivery. *J Biomater Sci Polym Ed.* **2018**, *29*, 1949-1963.
5. Yu, C.; Zhu, W.; He, Z.; Xu, J.; Fang, F.; Gao, Z.; Ding, W.; Wang, Y.; Wang, J.; Wang, J.; Huang, A.; Cheng, A.; Wei, Y.; Ai, S. ATP-triggered drug release system based on ZIF-90 loaded porous poly(lactic-co-glycolic acid) microspheres. *Colloids Surf Physicochem Eng Aspects.* **2021**, *615*, 126255.
6. Shi, X. D.; Sun, P. J.; Gan, Z.H. Preparation of porous polylactide microspheres and their application in tissue engineering. *Chin J Polym Sci.* **2018**, *36*, 712-719.
7. Seyyed Nasrollah, S. A.; Karimi-Soflou, R.; Karkhaneh, A. Photo-click crosslinked hydrogel containing MgO2-loaded PLGA microsphere with concurrent magnesium and oxygen release for bone tissue engineering. *Mater Today Chem.* **2023**, *28*, 101389.
8. Yuan, X.; Lin, S.; Zhao, K.; Han, Y. Emulsion-ultrasonic spray method to prepare polylactic acid microspheres. *Mater Lett.* **2022**, *309*, 131461.
9. Zeng, Y.; Li, X.; Liu, X.; Yang, Y.; Zhou, Z.; Fan, J.; Jiang, H. PLLA porous microsphere-reinforced silk-based scaffolds for auricular cartilage regeneration. *ACS Omega.* **2021**, *6*, 3372-3383.
10. Lin, A.; Liu, S.; Xiao, L.; Fu, Y.; Liu, C.; Li, Y. Controllable preparation of bioactive open porous microspheres for tissue engineering. *J Mater Chem B.* **2022**, *10*, 6464-6471.
11. Ali, W.; Ali, H.; Gillani, S.; Zinck, P.; Souissi, S. Polylactic acid synthesis, biodegradability, conversion to microplastics and toxicity: a review. *Environ Chem Lett.* **2023**, *21*, 1761-1786.
12. Amiryaghoubi, N.; Fathi, M.; Barar, J.; Omidian, H.; Omidi, Y. Hybrid polymer-grafted graphene scaffolds for microvascular tissue engineering and regeneration. *Eur Polym J.* **2023**, *193*, 112095.
13. Polyák, P.; Nagy, K.; Vértessy, B.; Pukánszky, B. Self-regulating degradation technology for the biodegradation of poly(lactic acid). *EnvironTechnol Innov.* **2023**, *29*, 103000.
14. Bee, S. L.; Hamid, Z. A. A.; Mariatti, M.; Yahaya, B. H.; Lim, K.; Bee, S. T.; Sin, L. T. Approaches to improve therapeutic efficacy of biodegradable PLA/PLGA microspheres: a review. *Polym Rev.* **2018**, *58*, 495-536.
15. Sahini, M. G. Polylactic acid (PLA)-based materials: a review on the synthesis and drug delivery applications. *Emergent Mater.* **2023**, *6*, 1461-1479.
16. Dodda, J. M.; Azar, M. G.; Bělský, P.; Šlouf, M.; Gajdošová, V.; Kasi, P. B.; Anerillas, L. O.; Kovářík, T. Bioresorbable films of polycaprolactone blended with poly(lactic acid) or poly(lactic-co-glycolic acid). *Int J Biol Macromol.* **2023**, *248*, 126654.
17. Bogdanova, A.; Pavlova, E.; Polyanskaya, A.; Volkova, M.; Biryukova, E.; Filkov, G.; Trofimenko, A.; Durymanov, M.; Klinov, D.; Bagrov, D. Acceleration of electrospun PLA degradation by addition of gelatin. *Int J Mol Sci.* **2023**, *24*, 3535.
18. Chen, Y.; Geever, L. M.; Killion, J. A.; Lyons, J. G.; Higginbotham, C. L.; Devine, D. M. Review of multifarious applications of poly (lactic acid). *Polym Plast Technol Eng.* **2016**, *55*, 1057-1075.
19. Swetha, T. A.; Ananthi, V.; Bora, A.; Sengottuvelan, N.; Ponnuchamy, K.; Muthusamy, G.; Arun, A. A review on biodegradable polylactic acid (PLA) production from fermentative food waste - Its applications and degradation. *Int J Biol Macromol.* **2023**, *234*, 123703.
20. Brunšek, R.; Kopitar, D.; Schwarz, I.; Marasović, P. Biodegradation properties of cellulose fibers and PLA biopolymer. *Polymers (Basel).* **2023**, *15*, 3532.
21. Shahdan, D.; Rosli, N. A.; Chen, R. S.; Ahmad, S.; Gan, S. Strategies for strengthening toughened poly(lactic acid) blend via natural reinforcement with enhanced biodegradability: A review. *Int J Biol Macromol.* **2023**, *251*, 126214.
22. Niu, Y.; Stadler, F. J.; Fu, M. Biomimetic electrospun tubular PLLA/gelatin nanofiber scaffold promoting regeneration of sciatic nerve transection in SD rat. *Mater Sci Eng C Mater Biol Appl.* **2021**, *121*, 111858.
23. Hou, Y.; Zhang, R.; Cheng, H.; Wang, Y.; Zhang, Q.; Zhang, L.; Wang, L.; Li, R.; Wu, X.; Li, B. Mg^{2+}-doped carbon dots synthesized based

on Lycium ruthenicum in cell imaging and promoting osteogenic differentiation in vitro. *Colloids Surf Physicochem Eng Aspects.* **2023**, *656*, 130264.
24. Zhu, S.; Dai, Q.; Yao, L.; Wang, Z.; He, Z.; Li, M.; Wang, H.; Li, Q.; Gao, H.; Cao, X. Engineered multifunctional nanocomposite hydrogel dressing to promote vascularization and anti-inflammation by sustained releasing of Mg^{2+} for diabetic wounds. *Compos B Eng.* **2022**, *231*, 109569.
25. Zhang, X.; Huang, P.; Jiang, G.; Zhang, M.; Yu, F.; Dong, X.; Wang, L.; Chen, Y.; Zhang, W.; Qi, Y.; Li, W.; Zeng, H. A novel magnesium ion-incorporating dual-crosslinked hydrogel to improve bone scaffold-mediated osteogenesis and angiogenesis. *Mater Sci Eng C Mater Biol Appl.* **2021**, *121*, 111868.
26. Zhu, Y.; Zhao, S.; Cheng, L.; Lin, Z.; Zeng, M.; Ruan, Z.; Sun, B.; Luo, Z.; Tang, Y.; Long, H. Mg^{2+}-mediated autophagy-dependent polarization of macrophages mediates the osteogenesis of bone marrow stromal stem cells by interfering with macrophage-derived exosomes containing miR-381. *J Orthop Res.* **2022**, *40*, 1563-1576.
27. Faisal, S.; Abdullah; Jan, H.; Shah, S. A.; Shah, S.; Rizwan, M.; Zaman, N.; Hussain, Z.; Uddin, M. N.; Bibi, N.; Khattak, A.; Khan, W.; Iqbal, A.; Idrees, M.; Masood, R. Bio-catalytic activity of novel mentha arvensis intervened biocompatible magnesium oxide nanomaterials. *Catalysts.* **2021**, *11*, 780.
28. Li, J.; Khalid, A.; Verma, R.; Abraham, A.; Qazi, F.; Dong, X.; Liang, G.; Tomljenovic-Hanic, S. Silk fibroin coated magnesium oxide nanospheres: a biocompatible and biodegradable tool for noninvasive bioimaging applications. *Nanomaterials (Basel).* **2021**, *11*, 695.
29. Welch, K.; Latifzada, M. A.; Frykstrand, S.; Strømme, M. Investigation of the antibacterial effect of mesoporous magnesium carbonate. *ACS Omega.* **2016**, *1*, 907-914.
30. Palominos, N.; Castillo, A.; Guerrero, L.; Borja, R.; Huiliñir, C. Coupling of anaerobic digestion and struvite precipitation in the same reactor: effect of zeolite and bischofite as Mg^{2+} source. *Front Environ Sci.* **2021**, *9*, 706730.
31. Hornak, J. Synthesis, properties, and selected technical applications of magnesium oxide nanoparticles: a review. *Int J Mol Sci.* **2021**, *22*, 12752.
32. Lin, Z.; Shen, D.; Zhou, W.; Zheng, Y.; Kong, T.; Liu, X.; Wu, S.; Chu, P. K.; Zhao, Y.; Wu, J.; Cheung, K. M. C.; Yeung, K. W. K. Regulation of extracellular bioactive cations in bone tissue microenvironment induces favorable osteoimmune conditions to accelerate in situ bone regeneration. *Bioact Mater.* **2021**, *6*, 2315-2330.
33. Fan, D.; De Rosa, E.; Murphy, M. B.; Peng, Y.; Smid, C. A.; Chiappini, C.; Liu, X.; Simmons, P.; Weiner, B. K.; Ferrari, M.; Tasciotti, E. Mesoporous silicon-PLGA composite microspheres for the double controlled release of biomolecules for orthopedic tissue engineering. *Adv Funct Mater.* **2012**, *22*, 282-293.
34. Yuan, Z.; Wei, P.; Huang, Y.; Zhang, W.; Chen, F.; Zhang, X.; Mao, J.; Chen, D.; Cai, Q.; Yang, X. Injectable PLGA microspheres with tunable magnesium ion release for promoting bone regeneration. *Acta Biomater.* **2019**, *85*, 294-309.
35. Wang, L.; Li, Y.; Jiang, S.; Zhang, Z.; Zhao, S.; Song, Y.; Liu, J.; Tan, F. Alginate hydrogels containing different concentrations of magnesium-containing poly(lactic-co-glycolic acid) microspheres for bone tissue engineering. *Biomed Mater.* **2023**, *18*, 055022.
36. Yuan, X.; Yang, W.; Fu, Y.; Tao, Z.; Xiao, L.; Zheng, Q.; Wu, D.; Zhang, M.; Li, L.; Lu, Z.; Wu, Y.; Gao, J.; Li, Y. Four-arm polymer-guided formation of curcumin-loaded flower-like porous microspheres as injectable cell carriers for diabetic wound healing. *Adv Healthc Mater.* **2023**, e2301486.
37. Hong, Y.; Gao, C.; Shi, Y.; Shen, J. Preparation of porous polylactide microspheres by emulsion-solvent evaporation based on solution induced phase separation. *Polym Adv Technol.* **2005**, *16*, 622-627.
38. Lee, H.; Nguyen, T. T.; Kim, M.; Jeong, J. H.; Park, J. B. The effects of biodegradable poly(lactic-co-glycolic acid)-based microspheres loaded with quercetin on stemness, viability and osteogenic differentiation potential of stem cell spheroids. *J Periodontal Res.* **2018**, *53*, 801-815.
39. Yang, S.; Liu, H.; Huang, H.; Zhang, Z. Fabrication of superparamagnetic magnetite/poly(styrene-co-12-acryloxy-9-octadecenoic acid) nanocomposite microspheres with controllable structure. *J Colloid Interface Sci.* **2009**, *338*, 584-590.
40. Pan, X.; Gao, M.; Wang, Y.; He, Y.; Si, T.; Sun, Y. Poly(lactic acid)-aspirin microspheres prepared via the traditional and improved solvent evaporation methods and its application performances. *Chin J Chem Eng.* **2023**, *60*, 194-204.
41. Schneider, C. A.; Rasband, W. S.; Eliceiri, K. W. NIH image to ImageJ: 25 years of image analysis. *Nat Methods.* **2012**, *9*, 671-675.
42. Rui, Y. F.; Lui, P. P.; Li, G.; Fu, S. C.; Lee, Y. W.; Chan, K. M. Isolation and characterization of multipotent rat tendon-derived stem cells. *Tissue Eng Part A.* **2010**, *16*, 1549-1558.
43. Livak, K. J.; Schmittgen, T. D. Analysis of relative gene expression data using real-time quantitative PCR and the 2(-Delta Delta C(T)) Method. *Methods.* **2001**, *25*, 402-408.
44. Liu, S.; Chen, W.; Xiao, L.; Zhao, Z.; Liu, F.; Lu, S.; Chen, C.; Luo, W.; Jiang, L.; Li, Y. Robust osteoconductive β-tricalcium phosphate/L-poly(lactic acid) membrane via orientation-strengthening technology. *ACS Biomater Sci Eng.* **2023**, *9*, 5293-5303.
45. Yuan, X.; Yang, W.; Fu, Y.; Tao, Z.; Xiao, L.; Zheng, Q.; Wu, D.; Zhang, M.; Li, L.; Lu, Z.; Wu, Y.; Gao, J.; Li, Y. Four-arm polymer-guided formation of curcumin-loaded flower-like porous microspheres as injectable cell carriers for diabetic wound healing. *Adv Healthc Mater.* **2023**, *12*, e2301486.
46. Lai, X. L.; Yang, W.; Wang, Z.; Shi, D. W.; Liu, Z. Y.; Yang, M. B. Enhancing crystallization rate and melt strength of PLLA with four-arm PLLA grafted silica: the effect of molecular weight of the grafting PLLA chains. *J Appl Polym Sci.* **2018**, *135*, 45675.
47. Lee, J. Y.; Kim, S. E.; Yun, Y. P.; Choi, S. W.; Jeon, D. I.; Kim, H. J.; Park, K.; Song, H. R. Osteogenesis and new bone formation of alendronate-immobilized porous PLGA microspheres in a rat calvarial defect model. *J Ind Eng Chem.* **2017**, *52*, 277-286.
48. Capuana, E.; Lopresti, F.; Ceraulo, M.; La Carrubba, V. Poly-l-lactic acid (PLLA)-based biomaterials for regenerative medicine: a review on processing and applications. *Polymers (Basel).* **2022**, *14*, 1153.
49. Zan, J.; Qian, G.; Deng, F.; Zhang, J.; Zeng, Z.; Peng, S.; Shuai, C. Dilemma and breakthrough of biodegradable poly-l-lactic acid in bone tissue repair. *J Mater Res Technol.* **2022**, *17*, 2369-2387.
50. Feng, P.; Shen, S.; Shuai, Y.; Peng, S.; Shuai, C.; Chen, S. PLLA grafting draws GO from PGA phase to the interface in PLLA/PGA bone scaffold owing enhanced interfacial interaction. *Sustain Mater Technol.* **2023**, *35*, e00566.
51. Yao, H.; Wang, J.; Deng, Y.; Li, Z.; Wei, J. Osteogenic and antibacterial PLLA membrane for bone tissue engineering. *Int J Biol Macromol.* **2023**, *247*, 125671.
52. Han, X.; Zhou, X.; Qiu, K.; Feng, W.; Mo, H.; Wang, M.; Wang, J.; He, C. Strontium-incorporated mineralized PLLA nanofibrous membranes for promoting bone defect repair. *Colloids Surf B Biointerfaces.* **2019**, *179*, 363-373.
53. Baek, S. W.; Kim, D. S.; Song, D. H.; Lee, S.; Lee, J. K.; Park, S. Y.; Kim,

J. H.; Kim, T. H.; Park, C. G.; Han, D. K. PLLA composites combined with delivery system of bioactive agents for anti-inflammation and re-endothelialization. *Pharmaceutics.* **2022**, *14*, 2661.

54. Shuai, Y. A tumor-microenvironment-activated nanoplatform of modified $SnFe_2O_4$ nanozyme in scaffold for enhanced PTT/PDT tumor therapy. *Heliyon.* **2023**, *9*, e18019.
55. Li, B.; Yang, H.; Cheng, K.; Song, H.; Zou, J.; Li, C.; Xiao, W.; Liu, Z.; Liao, X. Development of magnetic poly(L-lactic Acid) nanofibrous microspheres for transporting and delivering targeted cells. *Colloids Surf B Biointerfaces.* **2023**, *223*, 113175.
56. Wang, Y.; Zhao, L.; Zhou, L.; Chen, C.; Chen, G. Sequential release of vascular endothelial growth factor-A and bone morphogenetic protein-2 from osteogenic scaffolds assembled by PLGA microcapsules: A preliminary study in vitro. *Int J Biol Macromol.* **2023**, *232*, 123330.

Received: October 20, 2023
Revised: November 14, 2023
Accepted: November 25, 2023
Available online: December 28, 2023